

Original Article

## Network-based meta-analysis and confirmation of genes *ATP1A2*, *FXYD1*, and *ADCY3* associated with cAMP signaling in breast tumors compared to corresponding normal marginal tissues

Zahra Torki<sup>1,2</sup>, Davood Ghavi<sup>1,2</sup>, Zahra Foruzandeh<sup>3</sup>, Fatemeh Zeinali Sehrig<sup>3</sup>, Solmaz Hashemi<sup>4</sup>, Mohammad Reza Alivand<sup>1,5\*</sup>, Majid Pornour<sup>6,7\*</sup>

<sup>1</sup> Department of Medical Genetics, Faculty of Medicine, Tabriz University of Medical Sciences, Tabriz, Iran.

<sup>2</sup> Molecular Medicine Research Center, Biomedicine Institute, Tabriz University of Medical Sciences, Tabriz, Iran

<sup>3</sup> Department of Molecular Genetics, Ahar Branch, Islamic Azad University, Ahar, Iran

<sup>4</sup> General Surgery Department, Tabriz University of Medical Sciences, Tabriz, Iran

<sup>5</sup> Department of Biochemistry, Medical College of Wisconsin, Milwaukee, Wisconsin, USA

<sup>6</sup> Department of Photo Healing and Regeneration, Medical Laser Research Center, Yara Institute, Academic Center for Education, Culture, and Research (ACECR), Tehran, Iran;

<sup>7</sup> Department of Oncology, School of Medicine, University of Maryland, Maryland, USA

### Article Info

### Abstract



#### Article history:

**Received:** November 25, 2023

**Accepted:** August 16, 2024

**Published:** November 30, 2024

Use your device to scan and read the article online



Breast cancer (BC) is a global health concern with a growing prevalence. Since BC is a heterogeneous cancer, transcriptome analyzes were carried out on breast tumor tissues relative to their corresponding normal tissues in order to identify gene expression signatures and perform meta-analysis. Five expression profiling by array data sets from breast tumor tissues and non-tumor neighboring tissues were retrieved following a search in the GEO database (GSE70947, GSE70905, GSE10780, GSE29044, and GSE42568). Meta-analysis of gene expression using the Network Analyst tool identified common differentially expressed genes and biological pathways in all data sets. Then, the DEGs were analyzed through PPI network construction, gene ontology, and pathway analysis. The detected hub genes underwent Kaplan–Meier (KM) plotter and UALCAN validation. Finally, Real-time PCR analysis was used on BC patients' samples to determine mRNA levels of cAMP signaling pathway members *ATP1A2*, *FXYD1*, and *ADCY3*. Breast tumor tissues showed 710 differentially expressed genes (DEGs), with 392 overexpressed and 318 underexpressed, compared to normal marginal tissues. On the EnrichR library, GO, and KEGG pathway analyses were performed on the DEGs list. Progesterone-mediated oocyte maturation and the NF-kappa B signaling system were upregulated DEGs' top deregulated signaling pathways. In contrast, pathways related to cancer and the cAMP signaling pathway were the most enriched terms for down-regulated genes. Next, Real-time PCR quantification of cAMP signaling cascade members *ATP1A2*, *FXYD1*, and *ADCY3* was performed on 50 BC tumoral and non-tumoral tissues for validation. Results of meta-analyzed array data sets revealed DEGs representing BC gene signatures, and cAMP signaling pathway members as effective factors in BC. The results of our real-time PCR expression level determination for *ATP1A2*, *FXYD1*, and *ADCY3* in breast tumor tissues relative to the normal margins contradicted our bioinformatics investigations, which found increased levels for these genes. Of these, only *ATP1A2*'s expression levels were statistically significant. This study focused on identifying gene expression signatures that provide an invaluable source of evidence for BC-related underlying mechanisms to provide new therapeutic targets and biomarkers.

**Keywords:** cAMP signaling pathway, Breast cancer, GEO, Microarray

### 1. Introduction

Breast cancer is a global life-threatening issue with rising incidence [1, 2]. Due to the large degree of tumor heterogeneity, BC-related clinical outcomes vary amongst patients with different genetic subtypes or tumor features [3]. Multiple differentially expressed genes (DEGs) are responsible for the diverse molecular and cellular makeup of BC that collaborate to regulate cellular processes such

as cell differentiation, proliferation, and death [3, 4]. Knowing more about the expression patterns of the various tumor-driving DEGs of the primary tumor would be beneficial, given that the primary tumor is removed during treatments and that clinical decisions regarding the BC patient would be based on analyses of the primary tumor according to its histology and genetic components [5].

Microarray technology offers a high-throughput geno-

\* Corresponding author.

E-mail address: malivand@mcw.edu (MR Alivand); ma.pornour@gmail.com (M. Pornour).

Doi: <http://dx.doi.org/10.14715/cmb/2024.70.11.3>

mics tool for studying tumor-related expression patterns of multiple DEGs, providing insight into the genetic background, deriver mechanisms, and signaling pathways underlying disease development [5, 6]. Microarray studies' transcriptomic results are less reproducible due to variations in validation techniques, analysis methods, platforms, and sample collection and size [7]. To adress this problem, a series of statistical approaches using meta-analysis of microarray datasets have been used to discover sets of DEGs with robust expression signatures among tumors [8].

We conducted a meta-analysis on five BC microarray studies that compared the gene expression levels of breast tumor tissue with their matching normal margins and were published in the publicly accessible database Gene Expression Omnibus (GEO, <https://www.ncbi.nlm.nih.gov/geo/>). This was done considering the notion that integrating the results of numerous separate yet related research would potentially increase the repeatability of the results. Data integration in meta-analysis enhances gene signatures by increasing sample size, boosting statistical power, and eliminating biases from single experiments, resulting in robust and high-quality results [7]. In this regard, the NetworkAnalyst web platform (<https://www.networkanalyst.ca>) was used to integrate data from all the microarray gene expression data sets for transcriptome profiling, meta-analysis, and visualization of gene networks [9].

The goals of gene expression research are identification of molecular targets and determination of gene signatures as molecular alterations in disease genomes [10]. Gene signatures show unique expression patterns filtered through thousands of genes to predict disease outcomes and allocate molecular targets. These predictions require validation and are essential for disease diagnosis [10]. Finding the fundamental intercellular signaling mechanisms underpinning tumor progression is crucial [11]. The results of this study identified the cyclic adenosine monophosphate (cAMP) signaling pathway as a significant molecular alteration in breast tumors. Cell growth, migration, and mobility are indeed a few of the tumorigenic-related pathways that cAMP, a second messenger, regulates [12]. This cascade exhibits tumor-promoting and tumor-suppressive effects in various cancer types, requiring further investigation using clinical samples from BC patients [12].

DEGs from the meta-analysis were investigated using enrichment analyses, KEGG pathway, GO, bioinformatics, and real-time PCR on clinical samples to identify critical molecular pathways, deregulated gene signatures, and diagnostic biomarkers of BC. We performed bioinformatics validation on the hub genes. Also, clinical BC specimens were used for further validation of *ATPIA2*, *FXYD1*, and *ADCY3* expression levels in breast tumors. These genes were among the top ten most significantly down-regulated genes, and to the best of our knowledge, the expression levels of these genes (*ATPIA2*, *FXYD1*, and *ADCY3*) had never been confirmed in BC clinical samples by real-time PCR.

## 2. Materials and Methods

### 2.1. Acquiring eligible microarray datasets related to breast tumor tissue compared with their self-matching normal adjacent tissues

With the following phrases and their combination: "breast tumor tissue, breast adjacent normal tissue, pai-

red normal tissue, para tumor tissue, and gene expression profiling by array" as keywords, we systematically mined the National Center for Biotechnology Information (NCBI) GEO repository (<http://www.ncbi.nlm.nih.gov/geo/>) to collect publicly accessible microarray expression profiling datasets by May 2022. We carefully followed the previously established inclusion and exclusion criteria to gather the eligible datasets; in particular, we compiled a set of case and control studies comparing untreated human breast tumor tissue to the nearby normal tissues. These studies also had comparable conditions with the attainable raw and processed data. Studies with diverging designs or non-human sample populations were disqualified. Then, for each particular dataset, we extracted the following information: (1) GEO accession number (GSE code), (2) platform (GPL), (3) sample type (GSM), (4) gene expression data, and (5) number of cases and controls.

### 2.2. Data curation, annotation, and batch effect removal

For every individual data set, the gene expression matrix (GEM) as well as its related platform annotation files were retrieved and imported within the R statistical environment, using the "data.table" package's fread function [13]. Then, following Log2 transformation and data quality assessment through checking a uniform distribution among samples along with outlier identification with scanning boxplots, normalization of GEMs was conducted with the limma package's normalizaQuantile function [14]. By manually merging the probe ID columns of platform annotation files to the GEM table in R, the probe IDs were translated into the official gene symbols that correspond to them. The average value was taken into account for further analysis in cases of gene duplication (or several rows reporting the expression levels of the same gene).

Before data integration and meta-analysis with the NetworkAnalyst tool, batch effects (non-biological differences) across our chosen 5 studies were corrected using ComBat techniques to identify true biological variances in the gene expression profiles. Empirical Bayes techniques are used in the ComBat approach to stabilize gene expression ratios with very high or very low ratios and stabilize gene variances by minimizing variances among all genes, possibly protecting their inference from data artifacts [15]. Principal component analysis (PCA) was used to examine sample clustering patterns before and after this normalization as visual aids (Supplementary Data, Figure S1).

### 2.3. Data Network-based Meta-analysis

The gene expression meta-analysis on datasets related to the breast tumor tissue compared to normal marginal tissues (mentioned in Table 3) was carried out using the NetworkAnalyst 3.0 web tool (<https://www.networkanalyst.ca>), which is an online comprehensive meta-analysis and gene expression profiling platform [9]. After uploading all the individual annotated and normalized (preprocessed) datasets, we proceeded to the next step, which was to conduct ComBat normalization and PCA visualization for data integrity check. To extract differentially expressed genes (DEGs) from individual studies based on the Limma algorithm, NetworkAnalyst performs a Benjamini-Hochberg procedure and a moderated t-test resulting in an adjusted *P-value* (an adjusted *P-value* of less than 0.05 was considered statistically significant). Since

one of the meta-analysis approaches is combining effect size (ES), the integration of the results from combinable and comparable studies through which more biologically coherent results can be provided [16], we conducted the meta-analysis across breast tumor tissue and margin tissue to have DEGs among all independent data sets, proceeding with combining ES estimation, submitting the random effect size modeling (REM) statistical analysis. REM was chosen over fixed effect size modeling (FEM) since REM takes cross-study heterogeneity into account [17]. Using the Pattern extractor tool from NetworkAnalyst, a heatmap of all the DEGs and a volcano plot visualization of all the DEGs from meta-analysis results were provided.

#### 2.4. Network-based Protein-protein interaction (PPI) network construction and Hub gene detection

STRING (The Search Tool for the Retrieval of Interacting Genes) tool in the NetworkAnalyst application was applied to retrieve regulatory and functional networks of interactions among proteins, also known as protein-protein interactions (PPI) [18]. Briefly, gene symbols for up-regulated and down-regulated DEGs were uploaded to NetworkAnalyst's gene list input, with the highest confidence score cut-off and zero-order interaction option in PPI STRING. Hub genes, highly interconnected genes, were identified using NetworkAnalyst's hub explorer using degree and betweenness network centrality measures. Betweenness centrality measures the number of shortest paths through nodes, while Degree centrality measures the number of connections between nodes. [19].

#### 2.5. Signaling Pathway and Functional Enrichment Analysis

To explore highly enriched functions and pathways of the shared gene sets in breast tumors, Gene Ontology (GO) and KEGG pathway analyses were conducted on EnrichR online platform (<http://amp.pharm.mssm.edu/Enrichr/>) [20]. To get the list of significantly enriched annotations and pathways in EnrichR, we separately uploaded the official gene symbols of 318 down-regulated DEGs and 392 up-regulated DEGs to this web-based software, and then we subjected the DEGs to GO and KEGG pathway analyses. The enriched terms in GO and KEGG pathway analyses with a P-value < 0.05 were considered statistically significant. The GO annotation ('the latest version: GO-2023') provides information on the links between gene products and molecular functions (MF), biological process (BP), as well as cellular component (CC) type also, with performing a KEGG pathway analysis ('the latest version: KEGG-2021'), comes a better knowledge about the signaling cascades that shared deregulated gene sets in BT vs BNT take part in [21]. According to their P-value, the top 10 KEGG pathway and GO terms were sorted, and selection was based on a P-value < 0.05.

#### 2.6. Expression and Survival Analysis of Hub Genes and the Selected Genes from cAMP Signaling Using KM-plotter and UALCAN

The nine discovered hub genes and three genes related to the cAMP signaling cascade were subjected to survival analysis with Kaplan-Meier plotter (KM plotter) (<http://kmplot.com/analysis/>), a publicly available online software to evaluate their clinical prognostic significance. The following parameters were applied for determination

of the relapse-free survival (RFS) in 4929 samples of all breast cancer subtypes: relapse-free survival (RSF), split patient by median, follow-up threshold (all), censored at threshold (checked), invert HR values below 1 (not checked), compute median over entire database (false) and probe set option (user selected probe set). With the KM-plotter, the validation of the survival prognosis is facilitated by the evaluation of the correlation between the level of mRNA expression and survival in samples of 21 tumor types, including breast cancer [22].

To provide an in silico-analysis validation for the relative expression levels of nine hub genes as well as three selected genes from the cAMP signaling pathway in breast invasive carcinoma tumor tissues vs. normal ones, we explored an online web portal named UALCAN (<https://ualcan.path.uab.edu/>). This tool provides transcriptomic data, including the Cancer Genome Atlas (TCGA), to enable the evaluation of the relative expression level of genes in 33 tumors, including breast tumors [23].

#### 2.7. Patients and Clinical Specimens

We collected fifty pairs of breast tumor tissue specimens and their matching normal marginal tissues from patients diagnosed with BC who underwent surgery in Alzahra Hospital, Tabriz, Iran, from 2020 to 2022.

Following the protocols of Tabriz University of Medical Sciences Ethical Committee under the Ethics code of IR.TBZMED.REC.1400.1061, from newly diagnosed BC patients who gave us informed consent and had not undergone surgery or chemotherapy, tumor samples were excised and collected. From each BC patient, at least two samples were obtained, one tumor tissue and one to three distant marginal normal tissues (lateral, medial, and distal normal margins of the same tumor tissue). The procedure involved surgical dissection of breast tumor tissue and its corresponding distant pair from the same woman as the control sample in surgery, followed by freezing and storage at -80°C until further analysis. From each sample, one section was stained with Hematoxylin and Eosin for tumor cell presence confirmation. Table 1 shows the clinical pathological characteristics of BC patients who entered this study.

#### 2.8. Quantitative Polymerase Chain Reaction (qPCR) Expression Assay

The tissues were cut into smaller pieces and then homogenized with liquid nitrogen, then RNA extraction with TRIzol reagent (GeneAll) was followed. The quality and concentration of extracted RNAs were examined with the NanoDrop spectrometer (Thermo Scientific, USA) and gel electrophoresis. Lastly, by adding 50µl RNase-free water, purified RNAs were diluted and stored at -80°C. For the synthesis of complementary DNA (cDNA) according to the instructions of a first strand cDNA Reverse Transcriptase kit (KIAGENE FANAVAR, Iran), reverse transcriptase enzyme and buffer mix containing dNTPs were mixed. After that, a PCR cycle in the PCR Mastercycler Nexus - PCR Thermal Cycler machine (Eppendorf Mastercycler® Nexus, Germany) was performed according to the kit manufacturer's protocol as follows: 10 min at 25°C, 60 min at 47°C and 5 the last minute at 85°C to inactivate the enzyme.

To perform Real-time PCR to amplify the selected genes, cDNAs, specifically designed primers for *ATPIA2*,

*FXYD1*, *ADCY3* genes, and *GAPDH* as the endogenous reference gene for normalization of the real-time PCR data (Table 2 presents Primer sequences and their PCR product lengths) were used besides amplicon SYBR Green master mix (SMOBIO, Taiwan). We performed all the Real-Time PCR reactions with The Rotor-Gene Q (Qiagen, USA) machine in a 36-well plate in duplicate. The following cycling temperature condition was used: one initial hold step of 10 min at 95°C for template denature and enzyme activation for all the four genes, and the other three steps for every gene were 40 cycles as follows: for *ATP1A2*, *FXYD1*, and *GAPDH* 15 secs at 95°C, 30 secs at 60°C, and 30 secs at 72°C, for *ADCY3* 15 sec at 95°C, 30 secs at 62°C, and 30 secs at 72°C. Ultimately, for each gene, using the  $2^{-\Delta\Delta CT}$  and  $2^{-\Delta CT}$  methods, the average Ct was normalized to the control reference gene followed by a fold change (FC) calculation.

## 2.9. Statistical Analysis

To perform the meta-analysis in NetworkAnalyst 3.0, a random effects model (REM) with a significance level of  $<0.05$  was applied to the effect size (ES) combination. ES is defined as a standardized difference between means of groups divided by the standard deviation concerning both direction and magnitude of gene expression quantity. DEGs were determined using a  $P$ -value  $< 0.05$ . For functional enrichment and pathway analysis, a hypergeometric test with a threshold of  $P$ -value of  $< 0.05$  was considered statistically significant. In the survival plots generated by the KM-plotter database, hazard ratio (HR (with the corresponding confidence intervals)), log-rank,  $P$ -value, and median survivals were assessed and a log-rank  $p$ -value

less than 0.05 was considered statistically significant.

Real-time PCR expression analyzes were performed in duplicate and a paired Student's  $t$  test was used to calculate the relative expression of selected genes in breast tumor tissue compared to normal tissue using the delta Ct method.

R studio (4.1.3), REST (2009), and GraphPad Prism (version 6, San Diego, CA) software were used in this study. Survival analysis evaluation of hub genes by Kaplan–Meier plot was performed to obtain RFS curves. Throughout this study, a  $P$ -value  $< 0.05$  was the significance threshold.

## 3. Results

### 3.1. Selected Data Sets for The Meta-Analysis

Five studies were considered for our meta-analysis (GEO accession numbers: GSE70947, GSE70905, GSE10780, GSE29044, and GSE42568), due to the high quality of the metadata and compliance with the inclusion criteria (Table 3). 414 BC tumor mRNA expression profiles were downloaded to identify common transcription signatures, along with 391 non-tumorous adjacent tissues, as controls. Table 3 provides detailed descriptions of datasets, including accession numbers, platforms, sample types, and study types. GSE70947 and GSE70905 were subseries of GSE70951, involving expression profiling on paired breast adenocarcinoma and normal tissues using different Agilent platforms and samples. The other three gene sets were performed on the Affymetrix platform (GPL570, Affymetrix Human Genome U133 Plus 2.0 Array). We opted for studies that included over 50 samples, fresh frozen ones, and single-channel platforms. Only case/control stu-

**Table 1.** Baseline clinical characteristics of the 50 Breast cancer patients.

Characteristic		Number	percentage%
Age	50 ≤	38	76
	50 >	12	24
History of family cancer	Positive	18	36
	Negative	14	28
	NA	18	36
History of abortion	Positive	15	30
	Negative	17	34
	NA	17	34
Status of menopause	Positive	4	8
	Negative	44	88
	NA	2	4

**Table 2.** Real-time PCR specific forward and reverse primer sequences.

Gene name	Primer type	Primer sequence	Primer length	PCR product length (base pair)
ATP1A2	Forward	GATCATTGTGCCCACTTACCCT	22	149
ATP1A2	Reverse	CATTCCCAGTGCCTTCTAAGCC	22	
FXYD1	Forward	TGGGCATCCTCATCGTGCT	19	88
FXYD1	Reverse	GTTCCCTCCTCTTCATCGGGTT	22	
ADCY3	Forward	GGTATTGAGTGTCTGCGTTTCTT	23	114
ADCY3	Reverse	CATATACGTGCTGCCAATGGTTTT	24	
GAPDH	Forward	AAGGTGAAGGTCGGAGTCAAC	21	102
GAPDH	Reverse	GGGGTCATTGATGGCAACAA	20	

**Table 3.** Characteristics of microarray datasets included in the meta-analysis of breast tumor tissue vs. marginal normal tissue.

GEO accession code number (GSE)	Platform (GPL)	Number of Samples	Number of each Sample type		Experiment description	Publication Year and country	
			Breast tumor tissue	Marginal normal tissue			
GSE70951: A SuperSeries composing of the following SubSeries	GSE70905	Agilent-014850 Whole Human Genome Microarray 4x44K G4112F (GPL4133)	94	47	47	Age and estrogen-dependent inflammation in breast adenocarcinoma and normal breast tissue [cohort_1]	2015-USA
	GSE70947	Agilent-028004 SurePrint G3 Human GE 8x60K Microarray (GPL13607)	296	148	148	Age and estrogen-dependent inflammation in breast adenocarcinoma and normal breast tissue [cohort_2]	2015-USA
	GSE10780	[HG-U133_Plus_2] Affymetrix Human Genome U133 Plus 2.0 Array (GPL570)	185	42	143	Proliferative genes dominate malignancy-risk gene signature in histologically-normal breast tissue	2008-USA
	GSE29044	[HG-U133_Plus_2] Affymetrix Human Genome U133 Plus 2.0 Array (GPL570)	109	73	36	Expression data from breast tumors in different age-specific cohorts and for different sequential disease stages	2011-Saudi Arabia
	GSE42568	[HG-U133_Plus_2] Affymetrix Human Genome U133 Plus 2.0 Array (GPL570)	121	104	17	Breast Cancer Gene Expression Analysis	2012-Ireland

dies in breast tumor tissues compared with their respective normal margins or in breast tumor biopsies compared with normal biopsies were utilized. Using the online web-based platform NetworkAnalyst 3.0 (<https://www.networkanalyst.ca/>), the downstream data analysis was carried out in two stages: first, individual analysis to confirm the quality of datasets, and second, the meta-analysis to examine the expected differences in gene expression levels among all five data sets. The workflow of the present research is summarized in Figure 1, and more specific information on each data set, including the GEO accession code number (GSE), Platform (GPL), and Number of Samples, is provided in Table 3.

### 3.2. Batch Effect Adjustment

The ComBat method, a statistical option available in NetworkAnalyst, was used to solve problems related to non-biological conditions such as multi-platform studies with different samples and high levels of variability in laboratories.

Visualization of PCA plots indicated that before batch effect adjustment, the clustering pattern of Tumor samples vs. Normal samples from each data set were not as well distributed and intermixed as they were after batch effect adjustment (Supplementary Data, Figure S1).

### 3.3. Meta-Analysis Results of Shared DEGs Across Multiple Data-sets of Breast Tumor Tissue Compared to Their Corresponding Normal Adjacent Tissues

On NetworkAnalyst, the uploaded annotated and pre-processed datasets underwent a ComBat normalization, combining ES estimation and REM statistical analysis to

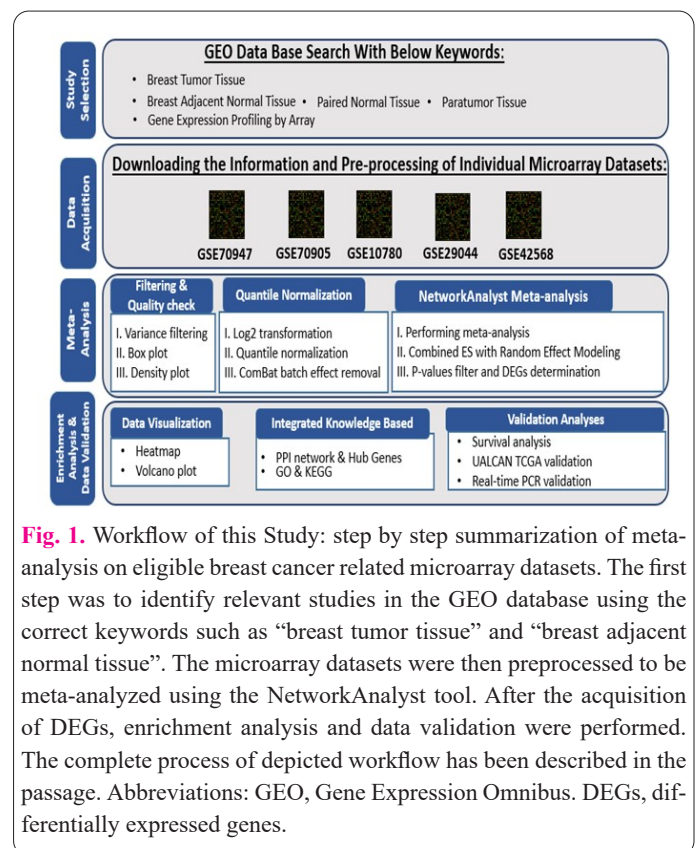


**Fig. 1.** Workflow of this Study: step by step summarization of meta-analysis on eligible breast cancer related microarray datasets. The first step was to identify relevant studies in the GEO database using the correct keywords such as “breast tumor tissue” and “breast adjacent normal tissue”. The microarray datasets were then preprocessed to be meta-analyzed using the NetworkAnalyst tool. After the acquisition of DEGs, enrichment analysis and data validation were performed. The complete process of depicted workflow has been described in the passage. Abbreviations: GEO, Gene Expression Omnibus. DEGs, differentially expressed genes.

detect the DEGs between breast tumor tissue and their corresponding normal tissues. When the total 1806 detected DEGs in the meta-analysis went under the statistical criteria (adjusted  $P$ -value < 0.05), the number of genes that

were screened out decreased to a total of 710 DEGs, of which 392 significantly overexpressed and 318 significantly underexpressed (adjusted P-value 0.05), (Supplementary Table 1 presents the DEGs from meta-analysis before and after considering the significance criteria). As presented in Table 4, Ubiquitin Like With PHD And Ring Finger Domains 1 (*UHRF1*), Enhancer Of Zeste 2 Polycomb Repressive Complex 2 (*EZH2*), Collagen Type X Alpha 1 Chain (*COL10A1*), and Centrosomal Protein 55 (*CEP55*) were the top significantly overexpressed and LIM Domain Binding 2 (*LDB2*), Heat Shock Protein Family B (Small) Member 2 (*HSPB2*), Glycine-N-Acyltransferase (*GLYAT*), Activin A Receptor Type 1C (*ACVR1C*), XYD Domain Containing Ion Transport Regulator 1 (*FXYD1*), and ATPase Na<sup>+</sup>/K<sup>+</sup> Transporting Subunit Alpha 2 (*ATP1A2*) were the top significantly down-regulated genes. The volcano plot in Figure 2. depicts the 392 significantly up-expressed DEGs and 319 significantly underexpressed DEGs among all the 1806 detected genes from the meta-analysis results. All the up- and down-regulated DEGs are presented in a heatmap and a volcano plot (Figure. 2 and Figure 3; Figure S2 in Supplementary Data). Both the volcano plot and heatmap figures were provided using the Pattern extractor tool from NetworkAnalyst.

### 3.4. Hub Genes Detected by Network-based Meta-Analysis

The STRING tool in the NetworkAnalyst website was used to build the PPI network of the 710 up-regulated and



**Fig. 2.** The volcano plot illustration of DEGs in breast tumor tissue in comparison to adjacent normal tissue in BC patients. Among the total number of 1806 detected shared genes from the meta-analyzed microarray data sets, 392 genes were significantly upregulated and 318 genes were significantly downregulated. The X- and Y-axis represent the log<sub>2</sub>-fold change (FC), -log<sub>10</sub> adjusted p-value respectively. Abbreviations: differentially expressed genes, DEGs; BC, breast cancer; fold change, FC.

down-expressed DEGs to understand the intricate connectivity among them. The zero-order network resulted in the large PPI network of all DEGs containing 126 nodes and 202 connecting edges. The force atlas layout was cho-

**Table 4.** Top 20 over- and under-expressed DEGs identified in the meta-analysis of breast tumor tissues vs. normal margin tissues. The ranking of DEGs were based on the combined effect size (ES). Abbreviations: DEGs, differentially expressed genes; ES, effect size.

Entrez ID	Official Gene Symbol	Gene Name	Combined ES	Adjusted P-Value
<b>Top 10 Upregulated genes in Breast tumor tissues vs normal margin</b>				
29128	UHRF1	Ubiquitin Like With PHD And Ring Finger Domains 1	2.0512	0.0018432
2146	EZH2	Enhancer Of Zeste 2 Polycomb Repressive Complex 2	1.9804	0.0044593
1300	COL10A1	Collagen Type X Alpha 1 Chain	1.9471	0.017245
55165	CEP55	Centrosomal Protein 55	1.8293	0.00019237
259266	ASPM	Assembly Factor For Spindle Microtubules	1.8039	0.0023289
3161	HMMR	Hyaluronan Mediated Motility Receptor	1.8	0.00016609
22974	TPX2	TPX2 Microtubule Nucleation Factor	1.7984	0.0038085
4751	NEK2	NIMA Related Kinase 2	1.7533	0.01807
9833	MELK	Maternal Embryonic Leucine Zipper Kinase	1.7472	0.00085722
9787	DLGAP5	DLG Associated Protein 5	1.6548	0.00082827
Entrez ID	Official Gene Symbol	Gene Name	Combined ES	Adjusted P-Value
<b>Top 10 downregulated genes in Breast tumor tissues vs normal margin tissues</b>				
9079	LDB2	LIM Domain Binding 2	-1.7922	8.09E-12
3316	HSPB2	Heat Shock Protein Family B (Small) Member 2	-1.7549	0.00071315
10249	GLYAT	Glycine-N-Acyltransferase	-1.714	0.0022982
130399	ACVR1C	Activin A Receptor Type 1C	-1.6853	0.0019864
5348	FXYD1	XYD Domain Containing Ion Transport Regulator 1	-1.5962	0.026828
477	ATP1A2	ATPase Na <sup>+</sup> /K <sup>+</sup> Transporting Subunit Alpha 2	-1.5941	0.0056164
9068	ANGPTL1	Angiopoietin Like 1	-1.5899	0.0063236
55273	TMEM100	Transmembrane Protein 100	-1.5866	1.55E-07
91851	CHRDL1	Chordin Like 1	-1.5671	0.004083
2908	NR3C1	Nuclear Receptor Subfamily 3 Group C Member 1	-1.5599	0.00047106

sen for a better visualization of the PPI network (Figure 4.). Ranked by degree, the top 10 hub genes were as follows: *PLK1*, *CCNB1*, *AURKA*, *ASPM*, *FYN*, *MCM2*, *JUN*, *KIF2C*, *KIF23*, and *RFC3* and Table 5 presents list of top ten hub genes based on network topology scores. The top three most highly ranked DEGs among hub genes were *PLK1* (Polo Like Kinase 1) with CombinedES of 1.0228 and an adjusted P-value of 0.045837, *AURKA* (Aurora Kinase A) with CombinedES of 1.3904 and an adjusted P-value of 0.030324 and *CCNB1* (Cyclin B1) with CombinedES of 1.6326 and an adjusted P-value of 0.0022068 (Supplementary Table 2: the complete list of nodes in the PPI network).

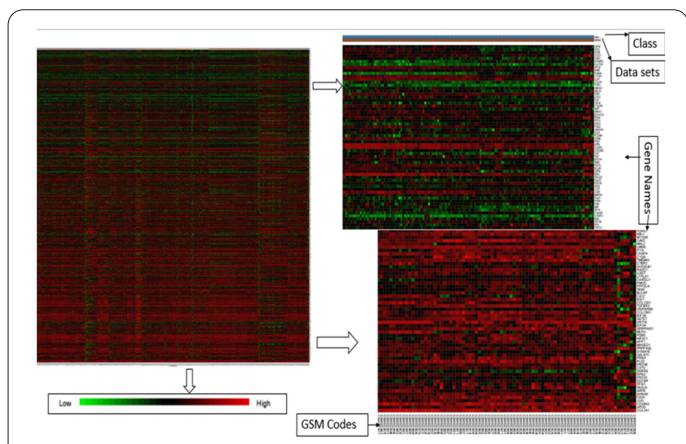


**Fig. 3.** (A) Heatmap of top 50 up- and down-regulated genes in all the data sets. (B) Heatmap of all 1806 genes resulted from the meta-analysis of all the microarray studies. Since the resulting picture was too big, the gene names that are presented on the right side of these heatmaps look blurred. The picture with the actual size is provided in the Supplementary Data file, Figure S2.

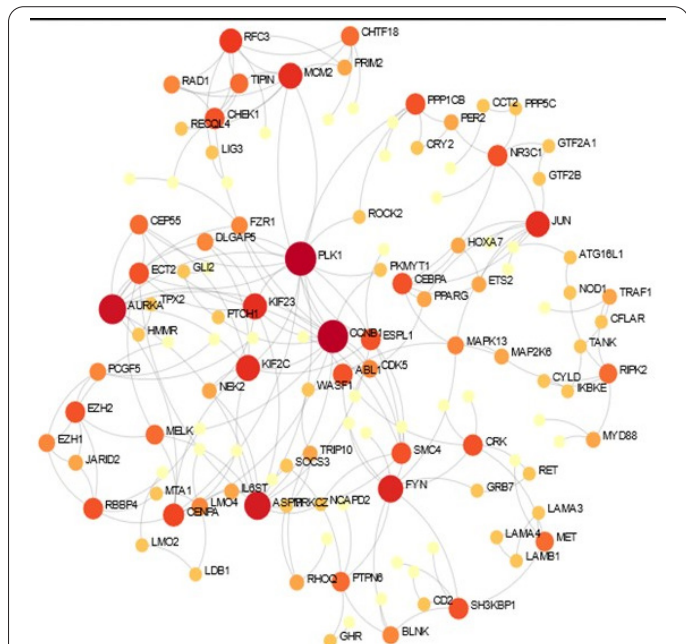


**Fig. 4.** Network-based analysis of the 710 DEGs in the meta-analysis. Detected hub genes via “Zero-order” protein-protein interaction network analysis of meta-analysis results of shred DEGs among breast tumor tissues relative to their corresponding normal tissues of BC patients. We used the Forced atlas layout of the subnetwork1. The bigger the node size in this figure, the higher the degree of the gene among all the hub genes of the resulting node table. Abbreviations: differentially expressed genes, DEGs; breast cancer, BC

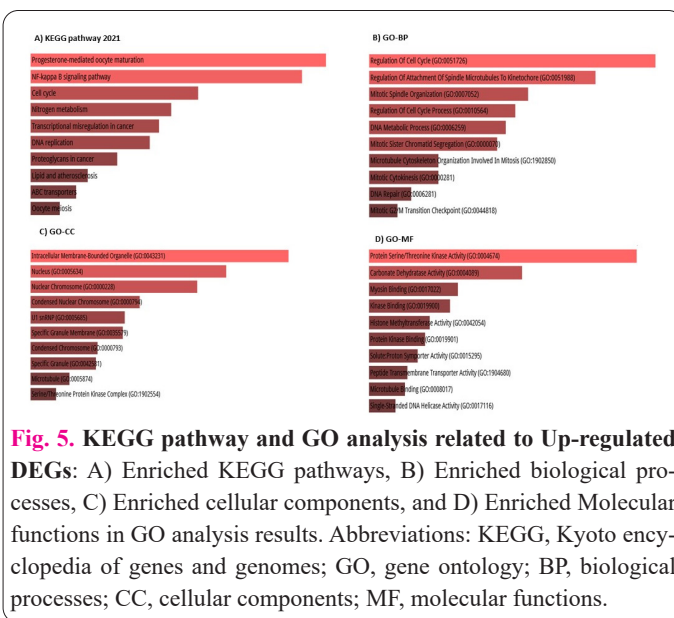


**Fig. 5.** KEGG pathway and GO analysis related to Up-regulated DEGs: A) Enriched KEGG pathways, B) Enriched biological processes, C) Enriched cellular components, and D) Enriched Molecular functions in GO analysis results. Abbreviations: KEGG, Kyoto encyclopedia of genes and genomes; GO, gene ontology; BP, biological processes; CC, cellular components; MF, molecular functions.

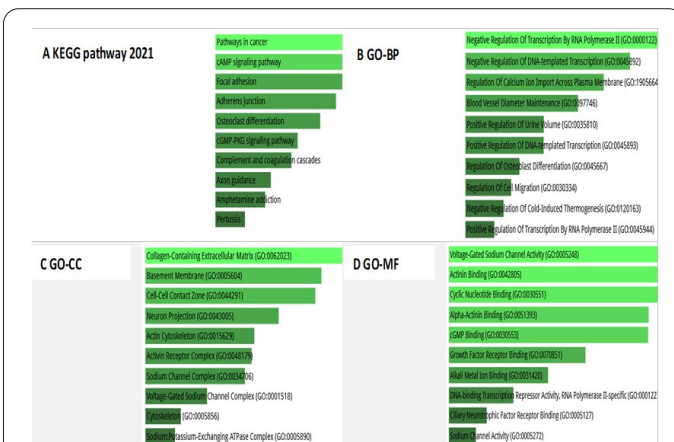


**Fig. 6.** KEGG pathway and GO analyses related to Down-regulated DEGs: A) Enriched KEGG pathways, B) Enriched biological processes, C) Enriched cellular components, and D) Enriched Molecular functions in GO analysis results. Abbreviations: KEGG, Kyoto encyclopedia of genes and genomes; GO, gene ontology; BP, biological processes; CC, cellular components; MF, molecular functions.

### 3.5. Functional Enrichment Annotation for Identification of Augmented Pathways and Gene Ontologies (GO)

Utilizing EnrichR online software, GO and KEGG pathway analyses were carried out to investigate the enriched GO keywords in the three BP, CC, and MF categories and to identify the significant signaling cascades connected to either down-expressed or up-expressed gene sets independently. Thus, the gene lists of 392 up-regulated gene groups and 318 down-regulated gene groups were subjected to GO and KEGG pathway extraction (Figure 5. shows GO and KEGG pathway analysis of the up-regulated genes and Figure 6. shows the same analysis of the down-expressed genes).

The latest GO (‘GO-2023) had three domains of ontologies: molecular function (MF), cellular component (CC), and biological process (BP) (Figures 5. and 6., a more detailed table of GO related to up-/down-expressed gene sets are provided in Supplementary Table 3). The top enriched terms of three GO categories were Protein Serine/Threonine Kinase Activity (MF), Intracellular Membrane-Bounded Organelle (CC) and Regulation Of Cell Cycle (BP) for

up-regulated genes and Voltage-Gated Sodium Channel Activity (MF), Collagen-Containing Extracellular Matrix (CC) and Negative Regulation Of Transcription By RNA Polymerase II (BP) for down-regulated genes.

For up-expressed genes the KEGG survey on EnrichR showed the most significant signaling pathway as Progesterone-mediated oocyte maturation and NF-kappa B signaling pathway (Figure 5A, Table 6), while for down-expressed genes pathways in cancer as well as cAMP signaling pathway were the most significantly enriched ones (Figure 6A, Table 7).

At this stage of our bioinformatics survey, to validate novel genes involved in breast tumor pathogenesis, we chose three genes from the cAMP signaling pathway for further validation by Real-time PCR since two DEGs from this pathway (*ATPIA2* and *FXYD1*) were among the top 10 down-regulated genes and a previous microarray study had shown a significant down-regulation for *ATPIA2* gene in breast cancer [24]. *ADCY3* was chosen as a candidate gene because it is involved in two major dysregulated pathways, including cancer pathways and the cAMP signaling pathway.

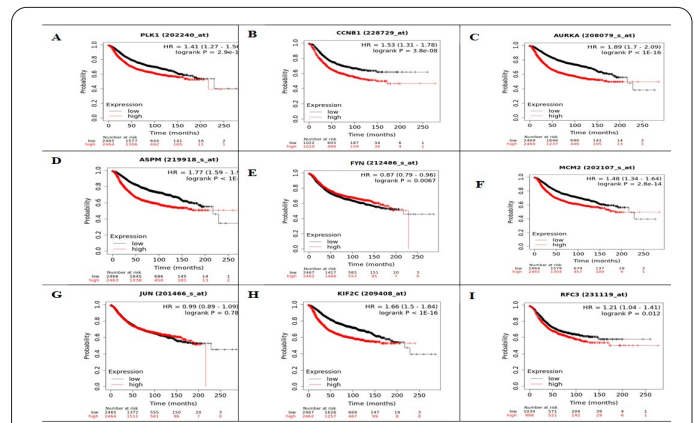


**Fig. 7.** KM plots based on relapse-free survival plots of 9 hub genes in patients with BC. Relapse-free survival (RFS) analysis of the following genes by low and high expression levels in BC patients: patients A) PLK1, B) CCNB1, C) AURKA, D) ASPM, E) FYN, F) MCM2, G) JUN, H) KIF2C, I) RFC3. For these genes higher expression is shown with a red line in the plot and the lower expression is shown with a black line in the plot. Abbreviations: KM plot, Kaplan-Meier plot; BC, breast cancer; HR (95% CI), hazard ratio (the corresponding 95% confidence intervals).

**Table 5.** The node table of hub genes with the degree of 8 or more from the network-based meta-analysis resulted DEGs.

Entrez ID	Gene	Full name	Degree	Betweenness	CombinedES	Adjusted P-Value
5347	PLK1	Polo Like Kinase 1	16	1047.25	1.0228	0.045837
891	CCNB1	Cyclin B1	15	3538.5	1.6326	0.002207
6790	AURKA	Aurora Kinase A	12	328.37	1.3904	0.030324
259266	ASPM	Assembly Factor For Spindle Microtubules	11	161.47	1.8039	0.0023289
2534	FYN	FYN Proto-Oncogene, Src Family Tyrosine Kinase	10	2119.25	-0.88733	0.0074117
4171	MCM2	Minichromosome Maintenance Complex Component 2	9	997.73	1.5123	0.00040627
3725	JUN	Jun Proto-Oncogene	9	780.39	-0.90239	0.015019
11004	KIF2C	Kinesin Family Member 2C	9	105.4	1.5954	0.0036374
5983	RFC3	Replication Factor C Subunit 3	8	376	0.66208	0.001243

**Table 6.** The obtained table from KEGG pathway analysis of the up-expressed DEGs results of the meta-analysis.

Term	P-value	Adjusted P-value	Odds Ratio	Combined Score	Genes
Progesterone-mediated oocyte maturation	7.86E-04	0.118400207	4.419384058	31.59471528	STK10;CCNB1;FZR1;RPS6KA1;PLK1;PKMYT1;AURKA;MAPK13
NF-kappa B signaling pathway	0.001016311	0.118400207	4.234375	29.18151747	BCL2A1;PLAU;BLNK;TRAF1;CCL19;MYD88;TNFSF13B;RELB
Cell cycle	0.003101988	0.202574821	3.500718391	20.21914101	CCNB1;FZR1;ESPL1;CHEK1;PLK1;PKMYT1;E2F5;MCM2
Nitrogen metabolism	0.004141963	0.202574821	10.79360999	59.22006374	CA12;CA2;CA9
Transcriptional misregulation in cancer	0.004721678	0.202574821	2.79414303	14.96428713	LDB1;BCL2A1;PLAU;MMP3;ASPSR1;ITGB7;TRAF1;PBX1;MEN1;BAIAP3
DNA replication	0.005216519	0.202574821	6.306701031	33.14754736	PRIM2;RFC3;DNA2;MCM2
Proteoglycans in cancer	0.007397742	0.24623913	2.606121627	12.78714541	COL1A1;VAV3;PLAU;CASP3;RPS6KB2;PLAUR;PTPN6;NUDT16L1;THBS1;MAPK13
Lipid and atherosclerosis	0.010155576	0.277032376	2.477716767	11.37205688	VAV3;CASP3;CCL5;MMP3;OLR1;TLR6;IKBKE;ABCG1;MYD88;MAPK13
ABC transporters	0.01150034	0.277032376	4.920040231	21.96984263	ABCD3;ABCC5;TAP1;ABCG1



**Table 7.** The obtained table from KEGG pathway analysis of the down-expressed DEGs results of the meta-analysis.

Term	P-value	Adjusted P-value	Odds Ratio	Combined Score	Genes
Pathways in cancer	1.48E-06	3.63E-04	3.233552321	43.41420024	CEBPA;CAMK2D;ROCK2;LAMA4;PTGER3;LAMA3;ADCY3;GLI2;EDNRB;PIM1;ABL1;BDKRB2;IL15RA;JUN;GSTM2;TCF7L1;ZBTB16;PTCH1;VEGFC;LAMB1;GSTA4;PPARG;IL6ST;MET;CRK
cAMP signaling pathway	9.99E-06	0.001228333	4.441115164	51.13625212	JUN;CAMK2D;NPR1;ROCK2;PTCH1;PTGER3;ADCY3;ATP1A2;PPP1CB;PDE10A;FXYD1;PPP1R1B;CNGA1;RAPGEF3
Focal adhesion	9.48E-05	0.007775813	4.044610437	37.46707297	PPP1CB;JUN;CAV2;ROCK2;PDGFD;LAMA4;LAMA3;VEGFC;FYN;LAMB1;CRK;MET
Adherens junction	1.34E-04	0.008229519	6.89417203	61.53635001	TCF7L1;FER;CSNK2A2;SNAI2;FYN;WASF1;MET
Osteoclast differentiation	1.99E-04	0.009794702	4.829027481	41.15204174	SOCS3;CYLD;PPP3CA;JUN;CALCR;FOSB;PPARG;FYN;MAP2K6
cGMP-PKG signaling pathway	3.51E-04	0.014405337	4.037761601	32.11525976	PPP1CB;PPP3CA;EDNRB;NPR1;ROCK2;BDKRB2;CNGA1;ADCY3;PDE5A;ATP1A2
Complement and coagulation cascades	4.11E-04	0.014445018	5.657020364	44.10680952	PROCR;C1QA;CFH;CFI;BDKRB2;SERPING1;C4BPA

### 3.6. Survival Analysis on KM Plotter and Expression Validation on UALCAN for Hub genes and *ATPIA2*, *FXYD1*, and *ADCY3* genes belonging to the cAMP Signaling

To confirm the association of hub genes with gene expression levels of *ATPIA2*, *FXYD1* and *ADCY3* and BC prognosis, we performed a survival analysis on the KM-plotter gene chip database [Breast] [25]. This analysis showed that high expression of *PLK1*, *CCNB1*, *AURKA*, *ASPM*, *MCM2*, *KIF2C*, and *RFC3* among the hub genes was significantly ( $\log$ -rank  $P < 0.05$ ) associated with poorer RFS in BC patients, while the lower expression of *FYN* had the same effect in BC patients (figure 7A to 7I). Furthermore, there was an association between shorter survival time and lower expression levels for *ATPIA2*, *FXYD1*, and *ADCY3* in BC patients (Figure 9A to 9C). The computation of HR and 95% confidence values was done automatically by the website. A narrower confidence interval report indicates a more precise survival possibility at every time point [26]. The hub genes and three selected genes of the cAMP signaling pathway were verified through data mining with the help from the UALCAN database. The agreement between the expression levels of these genes was confirmed by the BC TCGA scores and DEG scores on the meta-analyzed microarray data in this study. The expression levels of *PLK1*, *CCNB1*, *AURKA*, *ASPM*, *MCM2*, *KIF2C*, and *RFC3* had significant up-regulation. In contrast, *FYN* and *JUN* had significant down-expression in primary tumor compared to normal tissues in patients with breast invasive carcinoma (*BRCA*) (Figures 8A to 8I). The TCGA results for *ATPIA2*, *FXYD1*, and *ADCY3* also showed significant down-regulation in *BRCA* patients, similar to the results from the meta-analyzed studies and list of DEGs from our study (Figures 9D to 9F).  $P$ -value  $< 0.05$  was considered statistically significant.

### 3.7. Real-Time PCR Validation of Selected DEGs

#### 3.7.1. *ATPIA2* had a significantly increased level in breast tumor tissues

The results of paired T-test analysis revealed that the

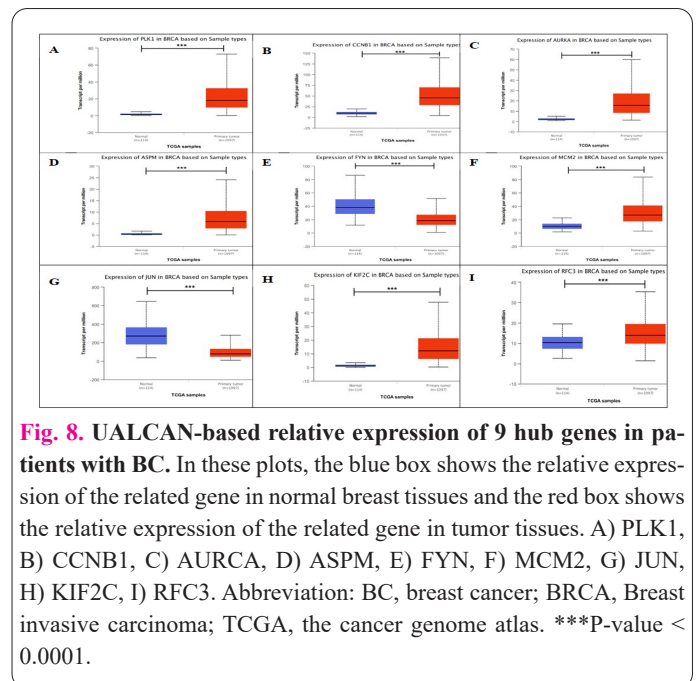


**Fig. 8.** UALCAN-based relative expression of 9 hub genes in patients with BC. In these plots, the blue box shows the relative expression of the related gene in normal breast tissues and the red box shows the relative expression of the related gene in tumor tissues. A) *PLK1*, B) *CCNB1*, C) *AURKA*, D) *ASPM*, E) *FYN*, F) *MCM2*, G) *JUN*, H) *KIF2C*, I) *RFC3*. Abbreviation: BC, breast cancer; *BRCA*, Breast invasive carcinoma; TCGA, the cancer genome atlas. \*\*\* $P$ -value  $< 0.0001$ .

expression level of *ATPIA2* was significantly increased in the breast tumor tissues compared with their normal marginal tissues ( $p$ -value = 0.016 and FC = 3.038) (Figure 10 A).

#### 3.7.2. *ADCY3* and *FXYD1* had non-significant increased levels in breast tumor tissues

*ADCY3* and *FXYD1*, although they had increased expression levels between breast tumor tissues and their corresponding normal tissues, the results were non-significant (FOR *FXYD1*:  $p$ -value = 0.654, and FC = 1.205 for and *ADCY3*:  $p$ -value = 0.300, and FC = 1.637) (Figure 10B and 10C respectively).

### 4. Discussion

In recent years, BC has accounted for the highest incidence of new female cancer cases, so targeting the progress of this disease seems urgent [27]. BC is a heteroge-

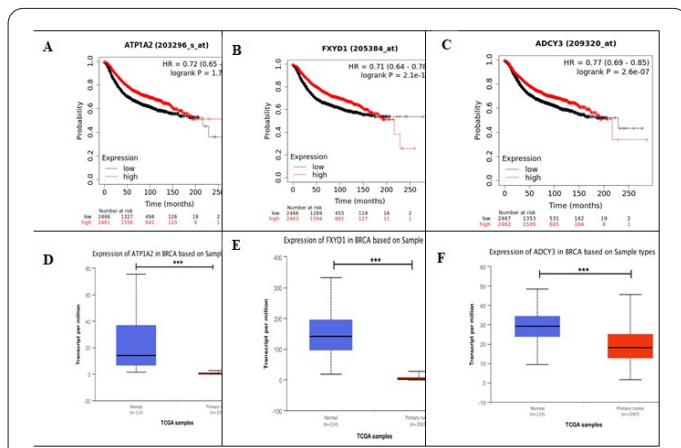


**Fig. 9.** KM plots based on relapse-free survival plots and UALCAN-based TCGA validation of three selected genes from the cAMP signaling pathway in patients with BC. Relapse-free survival (RFS) analysis of the following genes by low and high expression levels in BC patients: A) ATP1A2, B) FXYD1, C) ADCY3. UALCAN-based relative expression in normal tissues and breast cancer tissues: D) ATP1A2, E) FXYD1, F) ADCY3. Abbreviations: KM plot, Kaplan-Meier plot; BC, breast cancer, HR (95% CI), hazard ratio (the corresponding 95% confidence intervals). \*\*\*P-value < 0.0001.

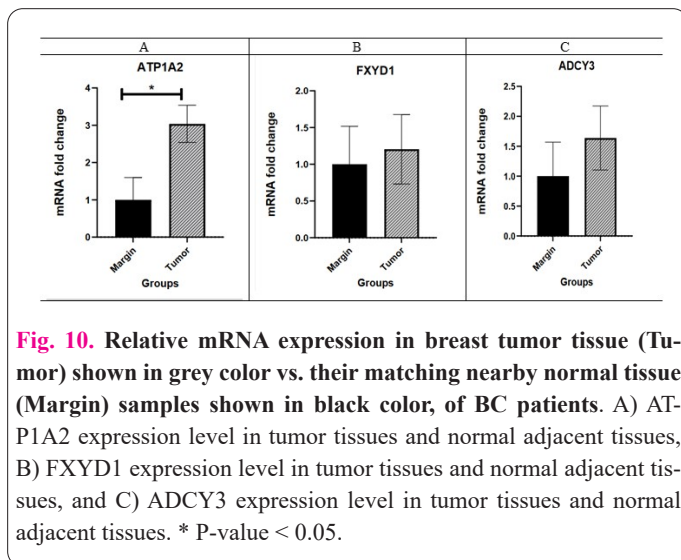


**Fig. 10.** Relative mRNA expression in breast tumor tissue (Tumor) shown in grey color vs. their matching nearby normal tissue (Margin) samples shown in black color, of BC patients. A) ATP1A2 expression level in tumor tissues and normal adjacent tissues, B) FXYD1 expression level in tumor tissues and normal adjacent tissues, and C) ADCY3 expression level in tumor tissues and normal adjacent tissues. \* P-value < 0.05.

neous group of diseases with divergences at the genomic, transcriptomic and epigenomic levels that explain the properties of tumor cell characteristics associated with the clinical outcome of the disease, including therapy resistance [28]. High-throughput technologies, such as microarrays, provide a better understanding of tumor characteristics by providing a platform to identify tumor transcriptome profiles [29]. One of the suggested methodologies that could discriminate breast tumor tissue from normal tissue is to detect robust DEG signatures that have addressable deregulations in breast tumor tissues [8]. A variety of statistical techniques are used in meta-analysis to produce a robust and reproducible signature of DEGs. Since gene expression profiling increases the likelihood of discovering the core molecular architecture and signaling pathways that explain the oncogenic characteristics of BC, we did a meta-analysis on five publicly accessible microarray studies in this study to understand BC at the molecular level. [30].

Microarray studies enable the parallel measurement

of gene expression levels on the whole genome breadth to improve our knowledge of cancer biology, treatment, and prognosis [31]. Gene expression profiles aid in optimal patient treatment selection based on disease severity, like molecular subtyping in breast cancer [32]. Despite the implications, these studies face hurdles like small sample size, data reproducibility, cross-platform comparisons, and statistical issues [31]. Meta-analysis integrates results from comparable studies using advanced statistical methodology, increasing observation count for statistical power in studies with similar design and purpose. In all, the sample size in our meta-analysis amounted to 805 breast tumor tissue samples and normal margins. We performed the meta-analysis on the NetworkAnalyst platform, which provides the ComBat normalization option as well as the REM method as a combining effect model that takes into account the cross-study heterogeneity that creates a robust gene signature of breast tumor tissue.

Under the significance cut-off of adjusted  $P$ -value < 0.05, 710 (392 significantly up-regulated and 318 significantly down-regulated) DEGs were identified after performing the meta-analysis on the five microarray studies across breast tumor tissues relative to normal margin tissues. The top 10 up-regulated DEGs are *UHRF1*, *EZH2*, *COL10A1*, *CEP55*, *ASPM*, *HMMR*, *TPX2*, *NEK2*, *MELK* and *DLGAP5*, and the top 10 down-regulated DEGs are *LDB2*, *HSPB2*, *GLYAT*, *ACVR1C*, *FXYD1*, *ATP1A2*, *ANGPTL1*, *TMEM100*, *CHRD1* and *NR3C1*. As brought in Table 4, among up-regulated DEGs, Ubiquitin Like With PHD And Ring Finger Domains 1 (*UHRF1*) showed the highest combined ES (2.0512). Previous studies have shown pro-invasion and pro-migration roles for this gene since *UHRF1* promoted BC cell proliferation, shortening the G1 phase and stimulating tumor vessel formation [33]. *UHRF1* is an epigenetic regulator and its overexpression has been demonstrated in many malignancies, including BC [34]. Consistent with our study, overexpression of Enhancer Of Zeste 2 Polycomb Repressive Complex 2 (*EZH2*) in BC has been reported in a microarray analysis that has introduced this gene as a marker of neoplastic transformation and aggressiveness of BC cells [35]. *EZH2* exhibits increased expression levels, particularly in advanced stages of BC. This gene is a subunit of histone methyltransferase enzyme in the polycomb repressive complex 2 (*PRC2*) [25] and it has been introduced as a biomarker of long-term metastatic risk, predicting metastasis in women with familial early-stage BC [36]. Up-regulated levels of Collagen Type X Alpha 1 Chain (*COL10A1*) (combinedES: 1.9471) reported in our study were in line with another study that reported its overexpression in all BC subtypes [37]. Higher expression levels of *COL10A1* predict a poor prognosis and tumor promotion in BC [38]. This gene was also introduced as a target for BC therapy and inhibition of this gene, curbed the cell migration properties of BC cells [38]. Centrosomal Protein 55 (*CEP55*) which showed a significantly elevated level in our study (combinedES: 1.8293), was introduced as a tumorigenic and genome destabilizing factor in an in vivo BC study [39]. Abnormal spindle-like microcephaly-associated (*ASPM*) gene was among both up-regulated (combinedES: 1.8039) and detected hub genes in a bioinformatics study related to BC. Its expression correlated with advanced grades of tumors, as it was found to be an up-regulate hub gene in this study as well [40]. *ASPM* encodes a spindle

protein is important for mitotic spindle function during cell replication [41]. Overexpression of *HMMR*, *TPX2*, *MELK*, *NEK2*, and *DLGAP5* was also shown in BC-related studies [42-46].

Among the down-regulated DEGs in this study, LIM Domain Binding 2 (*LDB2*, also called *CLIMI*) showed the lowest expression level in tumor vs. margin of BC tissues (combinedES: -1.7922). *LDB2* functions as a transcriptional regulatory factor that negatively affects tumor growth and migration in liver cancer and in BC cells, negatively affects the function of estrogen receptor-alpha (*ER α*) [47]. *ER α* controls signaling pathways that strongly influence the oncogenesis in mammary cells. Heat Shock Protein Family B (Small) Member 2 (*HSPB2*) is a member of the HSPs family that contributes to the maintenance of proteome functionality and is an ubiquitous ATP-independent chaperone [48]. Strong down-regulation of this gene was also observed in all subtypes (luminal A, luminal B, basal, Her2 enriched) of BC concordant with our study that showed a combinedES equal to -1.7549 [49]. Consistent with this result, down-expressed levels of *HSPB2* breast tumors vs. adjacent non-tumoral breast tissues were significant, and independent of the clinicopathological factors, higher expression of this gene indicates poor prognosis and relapse for BC patients [48]. Glycine N-acyltransferase (*GLYAT*), encoding an enzyme that produces coenzyme A (acyl-CoA) and acyl glycine, has down-regulated in BC tissues and cell lines, and its knockdown increased the proliferation rates *in vivo* and *in vitro*. The down-regulations of this gene induced PI3K/AKT/Snail pathway-related epithelial-mesenchymal transition (EMT), and an association of lower expression of *GLYAT* with poor prognosis for BC patients [50]. The expression levels of the top 10 up- and down-regulated genes in this study were not consistent with the results of the meta-analysis and were similar to the results of the UALCAN-derived TCGA expression levels of the DEGs (Supplementary Data, Table S1).

The list of DEGs underwent network-based meta-analysis to detect the hub genes. Among the resulting hub genes, there was a link between Polo Like Kinase 1 (*PLK1*) and Aurora Kinase A (*AURKA*) in cell cycle progression through entering mitosis and assembly of spindle [51]. Both of these genes had significantly higher expression levels in breast tumor tissues in our meta-analysis of this study and other studies on BC [52]. In TNBC, targeting *PLK1* by BI-2536, a selective inhibitor for this protein, is introduced as a warranted targeted therapy [53]. Cyclin B1 (*CCNB1*) was also introduced as a promising biomarker for ER<sup>+</sup> BC prognosis, a target for BC prevention and reversion of therapy resistance [54]. It was shown that inhibition of *CCNB1* decreases the proliferation of the cells, arrests the cells in the G2/M phase, and opposes the EMT mechanism [55]. The Assembly Factor For Spindle Microtubules (*ASPM*), encoded by primary microcephaly 5 (*MCPH5*), plays an essential role in ensuring spindle position during mitosis and controlling DNA replication and has been associated with a poor prognosis in BC [40]. *FYN* Proto-Oncogene, Src Family Tyrosine Kinase (*FYN*) is a member of the Src family of kinases (SFKs) which in our study showed significant down-regulation (combinedES -0.88733), has indicated an overexpression in BC, as well as promotion of migration, invasion, and proliferation in BC cell, lines [56]. Members of this family include

*Src*, *FYN*, and *YES* that play essential roles in several signaling pathways such as cell proliferation [57]. Other hub genes including *MCM2*, *KIF2C* and *RFC3* also showed increased expression in BC [58, 59]. Jun Proto-Oncogene (*JUN*) encodes the c-Jun transcription factor, which plays an essential role in tumor metastasis and showed decreased expression in this study (combinedES: -0.90239). This gene can play tumor suppressor and oncogenic roles in cancer [60].

KM-plotter analysis was performed on the hub genes to determine their prognostic value. Relapse-free survival (RFS) KM-plotter showed a significantly lower survival probability of patients with increased expression levels of *PLK1*, *CCNB1*, *AURKA*, *ASPM*, *MCM2*, *KIF2C*, and *RFC3* but decreased levels of *FYN* had the same effect in BC patients. We also performed a comparison of gene expression levels between tumor and normal tissues of the BC dataset using TCGA analysis in the UALCAN database. The results were consistent with our survey.

In this study, we conducted GO and KEGG pathway analysis to unveil the deregulated molecular functions and signaling pathways underlying BC tumorigenesis. The results of GO and KEGG pathway analysis were consistent for both up-regulated and down-regulated DEGs. KEGG pathway analysis the DEGs of the up-regulated list indicated that Progesterone-mediated oocyte maturation, NF-kappa B signaling pathway, and Cell cycle signaling pathways were associated with the pathogenesis of BC. This result was consistent with another study on BC [61]. Progesterone is essential in BC carcinogenesis and induces cellular proliferation in the mammary epithelium in the presence of estrogen [62]. When we explored the KEGG signaling pathways for down-expressed DEGs the results included Pathways in cancer, cAMP signaling pathway, Focal adhesion, and Adherence junction. The expression of members of these signaling pathways showed reduced levels and these genes are related to the connections of tumor cells with each other. They may represent the entering of the tumor into an invasive mode into a definitive metastasis. A study on BC showed that activation of the cAMP signaling pathway leads to inhibition of BC cell migration [63]. cAMP is a second messenger acting as an important mediator of several cellular functions including cellular proliferation, migration, and invasion [64]. Interestingly, Estrogen hormones have been shown to increase the cAMP levels, as well as their direct interaction with chromosomes; as a result, estrogen hormone-mediated changes in gene expression levels may involve the activation of cAMP [65]. Because it is an important but not extensively studied signaling pathway, we selected three genes from the cAMP signaling pathway for further investigation in clinical BC specimens. The other genes involved in the GO and KEGG pathways should be investigated in more detail in the future.

*ATP1A2*, *FXYD1*, and *ADCY3* were all members of the three major down-regulated signaling cascades, whose expression levels have not been previously examined in clinical BC samples. According to the meta-analysis results, all three genes were significantly down-regulated in breast tumors (combinedESs for *ATP1A2*, -1.5941; *FXYD1*, -1.5962; *ADCY3*, -0.52862). Comparison of TCGA expression level between breast tumors and normal tissue also showed significant down-expression based on UALCAN-Web. KM plotter analysis of these genes showed signifi-

cantly increased recurrence-free survival in patients with increased expression of these genes. Further microarray expression level determination for ATP1A2 also showed significant down-regulation in BC, but ATP1A1 (coding  $\alpha 1$  subunit) showed increased expression [24].

In contrast to our bioinformatics studies, after performing real-time PCR expression level determination for ATP1A2, FXYD1 and ADCY3 in breast tumor tissues compared to the normal margins, we observed increased levels for these genes, where only the expression levels of ATP1A2 reached statistical significance. ATP1A2 gene encodes the  $\alpha 2$ -subunit of the Na<sup>+</sup>/K<sup>+</sup> ATPase (NKA) that is a member of p-class pumps. NKA is a hetero-oligomeric protein that is composed of three sub-units ( $\alpha$ ,  $\beta$ , and  $\gamma$ ). The  $\alpha$  and  $\beta$  subunits are catalytic, and the  $\gamma$  subunit consists of the FXYD family (FXYD1-7) [66]. ADCY3 catalysis is involved in the production of cAMP, a membrane-associated protein. Its overexpression has a tumorigenesis function in gastric cancer, but we couldn't find any study on the function and expression levels of this gene in BC [67].

Not only does NKA act as an ionic pump, but it also acts as a signal transducer and membrane receptor [66]. FXYD1 encodes phospholamban (PLM) protein that interacts with and regulates NKAs [68]. A review study reported an association of NKA with diverse cellular functions like proliferation and survival as well as cell death. This pump is also involved in cell adhesion and cellular invasion [66]. When there is deregulation of the  $\alpha$ ,  $\beta$ , and  $\gamma$  subunits of the NKAs, cell adhesion decreases and cell migration increases [66].

So, since different studies have reported diverse and sometimes opposite functions for this protein, the contrast that we noted in this study might be because the up-regulated pathways induced cell proliferation and down-expressed pathways showed a lowering in the cellular adhesion, in our study with samples of BC patients, the invasive function of NKA was activated. We speculate that the contrast between our bioinformatics and clinical samples expression level determination is due to the differences in the stages and sampling conditions of our study from the ones of microarray surveys.

This study, like any other, has several strengths and limitations, and its acknowledgment would shed light on future studies. First, dataset and platform heterogeneity and confounding factors might have skewed our statistical analysis. To solve this issue, we performed batch effect correction by normalization for each data set well as before performing the meta-analysis on NetworkAnalyst, and we had common platforms for three data sets (GSE10780, GSE29044 and GSE42568) and the other two were sub-series of a more extensive study (GSE70905, GSE70947). Second, the sample size for meta-analysis was not adequate since we examined the expression levels of thousands of genes. Due to the heterogeneity of BC subtypes, a better approach to the detect DEGs for BC patients should also consider the subtypes of this disease. It is worth mentioning that another limitation of the sampling subject would be the notion that ethnicity is an important confounding factor in this study. Also for our real-time PCR validation experiments, we only studied the expression levels of three genes on a small sample size for BC patients. Third, our bioinformatics results from the meta-analyzed DEGs were consistent with the TCGA results, but the expression

levels of ATP1A2, FXYD1, and ADCY3 had discordance levels in samples from BC patients. Last but not least, we did not provide more experimental studies for our survey due to the limitations in financial and laboratory equipment. We suggest more extensive experimental studies on this subject, especially on the NKA protein function in BC.

## 5. Conclusions

Taken together this study reported an integrative meta-analysis on five microarray data sets related to BC, comparing the mRNA levels of shared DEGs among these studies using the NetworkAnalyst online tool. The list of DEGs obtained from the meta-analysis underwent PPI, hub gene detection, GO, and pathway analysis to gain more insight into the primary molecular factors affecting BC pathogenesis. cAMP signaling pathway was among the most significantly deregulated pathways related to the down-expressed DEGs, and the expression levels of three members of this cascade were surveyed in BC patients' derived tumor tissues relative to their corresponding normal ones. The hub genes were also under survival and expression analysis in BC patients through a bioinformatics database named UALCAN. To the best of our knowledge, this study was the first to identify the expression level of the selected three DEGs from the cAMP signaling pathway, namely ATP1A2, FXYD1 and ADCY3. This project also provided the other signaling pathways, PPIs, gene ontology terms and a list of DEGs for future biomarker determination and prognostic studies.

## Abbreviations

ADCY3 (*Adenylate Cyclase 3*)

ATPIA2 (*ATPase Na<sup>+</sup>/K<sup>+</sup> Transporting Subunit Alpha 2*)

BC (*Breast Cancer*)

BP (*Biological Process*)

CC (*cellular component*)

cDNA (*complementary DNA*)

cAMP (*cyclic Adenosine Mono Phosphate*)

Ct (*Cycle threshold*)

DEGs (*Differentially Expressed Genes*)

ES (*Effect Size*)

FXYD1 (*FXYD Domain Containing Ion Transport Regulator 1*)

GAPDH (*Glyceraldehyde-3-phosphate dehydrogenase*)

GO (*Gene Ontology*)

GEO (*Gene Expression Omnibus*)

KEGG (*Kyoto Encyclopedia of Genes and Genomes*)

KM-Plotter (*Kaplan-Meier plotter*)

NCBI (*National Center for Biotechnology Information*)

PPI (*Protein-Protein Interaction*)

REM (*Random Effect Modeling*)

REST (*Relative Expression Software Tool*)

SYBR Green (*asymmetrical cyanine dye used as a nucleic acid stain*)

TCGA (*The Cancer Genome Atlas*)

## Conflict of Interests

The authors declare that they have no conflict of interest.

## Consent for publications

The authors read and approved the final manuscript for publication.

### Ethics approval and consent to participate

The Ethics Committee of Tabriz University of Medical Sciences, Tabriz, Iran approved this study with the Ethics Code IR.TBZMED.REC.1400.1061.

### Informed Consent

Informed consent was obtained from all patients who participated in our study.

### Availability of data and material

The data that support the findings of this study are available from the corresponding authors upon reasonable request. Also, at <https://www.ncbi.nlm.nih.gov/GEO> the analysed datasets that this study used are available and the supplementary data provides more details.

### Authors' contributions

MA and MP: Research design and supervision of the experiments and manuscript revision; ZT: study conduction, data and sample collection and meta-analysis, and writing the first draft of the manuscript; DG, ZF, and FS and SH: sample collection and contribution in study conduction; Authors read and approved the final version of the manuscript.

### Funding

This study was supported through the Molecular Medicine Research Center (Grant No. 69015) of Tabriz University of Medical Sciences, Tabriz, Iran.

### Acknowledgment

We appreciate the efforts of the Medical Genetic lab staff at the Department of Medical Genetics, the Molecular Medicine Research Center, and the medical staff at Alzahra Hospital.

### References

- Hajibabaei S, Nafissi N, Azimi Y, Mahdian R, Rahimi-Jamrani F, Valizadeh V, Rafiee MH, Azizi M (2023) Targeting long non-coding RNA MALAT1 reverses cancerous phenotypes of breast cancer cells through microRNA-561-3p/TOP2A axis. *Sci Rep* 13 (1): 8652. doi: 10.1038/s41598-023-35639-x
- Ali Salman R (2023) Prevalence of women breast cancer. *Cell Mol Biomed Rep* 3(4): 185-196. doi: 10.55705/cmbr.2023.384467.1095
- Sørli T, Perou CM, Tibshirani R, Aas T, Geisler S, Johnsen H, Hastie T, Eisen MB, van de Rijn M, Jeffrey SS, Thorsen T, Quist H, Matese JC, Brown PO, Botstein D, Lønning PE, Børresen-Dale AL (2001) Gene expression patterns of breast carcinomas distinguish tumor subclasses with clinical implications. *Proc Natl Acad Sci U S A* 98 (19): 10869-10874. doi: 10.1073/pnas.191367098
- Seif F, Torki Z, Zalpoor H, Habibi M, Pornour M (2023) Breast cancer tumor microenvironment affects Treg/IL-17-producing Treg/Th17 cell axis: Molecular and therapeutic perspectives. *Mol Ther Oncolytics* 28: 132-157. doi: 10.1016/j.omto.2023.01.001
- Fischer JR, Jackson HW, de Souza N, Varga Z, Schraml P, Moch H, Bodenmiller B (2023) Multiplex imaging of breast cancer lymph node metastases identifies prognostic single-cell populations independent of clinical classifiers. *Cell Rep Med* 4 (3): 100977. doi: 10.1016/j.xcrm.2023.100977
- Soheilifar MH, Vaseghi H, Seif F, Ariana M, Ghorbanifar S, Habibi N, Papari Barjasteh F, Pornour M (2021) Concomitant overexpression of mir-182-5p and mir-182-3p raises the possibility of IL-17-producing Treg formation in breast cancer by targeting CD3d, ITK, FOXO1, and NFATs: A meta-analysis and experimental study. *Cancer Sci* 112 (2): 589-603. doi: 10.1111/cas.14764
- Savino A, De Marzo N, Provero P, Poli V (2021) Meta-Analysis of Microdissected Breast Tumors Reveals Genes Regulated in the Stroma but Hidden in Bulk Analysis. *Cancers (Basel)* 13 (13). doi: 10.3390/cancers13133371
- Gur-Dedeoglu B, Konu O, Kir S, Ozturk AR, Bozkurt B, Ergul G, Yulug IG (2008) A resampling-based meta-analysis for detection of differential gene expression in breast cancer. *BMC Cancer* 8: 396. doi: 10.1186/1471-2407-8-396
- Zhou G, Soufan O, Ewald J, Hancock REW, Basu N, Xia J (2019) NetworkAnalyst 3.0: a visual analytics platform for comprehensive gene expression profiling and meta-analysis. *Nucleic Acids Res* 47 (W1): W234-w241. doi: 10.1093/nar/gkz240
- Mallik S, Zhao Z (2018) Identification of gene signatures from RNA-seq data using Pareto-optimal cluster algorithm. *BMC Syst Biol* 12 (Suppl 8): 126. doi: 10.1186/s12918-018-0650-2
- Ahmed MB, Alghamdi AAA, Islam SU, Lee JS, Lee YS (2022) cAMP Signaling in Cancer: A PKA-CREB and EPAC-Centric Approach. *Cells* 11 (13). doi: 10.3390/cells11132020
- Zhang H, Kong Q, Wang J, Jiang Y, Hua H (2020) Complex roles of cAMP-PKA-CREB signaling in cancer. *Exp Hematol Oncol* 9 (1): 32. doi: 10.1186/s40164-020-00191-1
- Huber W, Carey VJ, Gentleman R, Anders S, Carlson M, Carvalho BS, Bravo HC, Davis S, Gatto L, Girke T, Gottardo R, Hahne F, Hansen KD, Irizarry RA, Lawrence M, Love MI, MacDonald J, Obenchain V, Oleś AK, Pagès H, Reyes A, Shannon P, Smyth GK, Tenenbaum D, Waldron L, Morgan M (2015) Orchestrating high-throughput genomic analysis with Bioconductor. *Nat Methods* 12 (2): 115-121. doi: 10.1038/nmeth.3252
- Ritchie ME, Phipson B, Wu D, Hu Y, Law CW, Shi W, Smyth GK (2015) limma powers differential expression analyses for RNA-sequencing and microarray studies. *Nucleic Acids Research* 43 (7): e47-e47. doi: 10.1093/nar/gkv007
- Zhang Y, Parmigiani G, Johnson WE (2020) ComBat-seq: batch effect adjustment for RNA-seq count data. *NAR Genomics and Bioinformatics* 2 (3). doi: 10.1093/nargab/lqaa078
- Siangphoe U, Archer KJ (2017) Estimation of random effects and identifying heterogeneous genes in meta-analysis of gene expression studies. *Brief Bioinform* 18 (4): 602-618. doi: 10.1093/bib/bbw050
- Borozan I, Chen L, Paeper B, Heathcote JE, Edwards AM, Katze M, Zhang Z, McGilvray ID (2008) MAID: An effect size based model for microarray data integration across laboratories and platforms. *BMC Bioinformatics* 9 (1): 305. doi: 10.1186/1471-2105-9-305
- Szklarczyk D, Kirsch R, Koutrouli M, Nastou K, Mehryary F, Hachilif R, Gable AL, Fang T, Doncheva NT, Pyysalo S, Bork P, Jensen LJ, von Mering C (2023) The STRING database in 2023: protein-protein association networks and functional enrichment analyses for any sequenced genome of interest. *Nucleic Acids Res* 51 (D1): D638-d646. doi: 10.1093/nar/gkac1000
- Soofi A, Taghizadeh M, Tabatabaei SM, Rezaei Tavirani M, Shakib H, Namaki S, Safari Alighiarloo N (2020) Centrality Analysis of Protein-Protein Interaction Networks and Molecular Docking Prioritize Potential Drug-Targets in Type 1 Diabetes. *Iran J Pharm Res* 19 (4): 121-134. doi: 10.22037/ijpr.2020.113342.14242
- Chen EY, Tan CM, Kou Y, Duan Q, Wang Z, Meirelles GV, Clark NR, Ma'ayan A (2013) Enrichr: interactive and collaborative HTML5 gene list enrichment analysis tool. *BMC Bioinformatics* 14 (1): 128. doi: 10.1186/1471-2105-14-128
- Kanehisa M, Furumichi M, Tanabe M, Sato Y, Morishima K (2017) KEGG: new perspectives on genomes, pathways, diseases

- and drugs. *Nucleic Acids Res* 45 (D1): D353-d361. doi: 10.1093/nar/gkw1092
22. Györfy B (2023) Discovery and ranking of the most robust prognostic biomarkers in serous ovarian cancer. *Geroscience*. doi: 10.1007/s11357-023-00742-4
  23. Chandrashekar DS, Bachel B, Balasubramanya SAH, Creighton CJ, Ponce-Rodriguez I, Chakravarthi B, Varambally S (2017) UALCAN: A Portal for Facilitating Tumor Subgroup Gene Expression and Survival Analyses. *Neoplasia* 19 (8): 649-658. doi: 10.1016/j.neo.2017.05.002
  24. Bogdanov A, Moiseenko F, Dubina M (2017) Abnormal expression of ATP1A1 and ATP1A2 in breast cancer. *F1000Res* 6: 10. doi: 10.12688/f1000research.10481.1
  25. Adibfar S, Elveny M, Kashikova HS, Mikhailova MV, Farhangnia P, Vakili-Samiani S, Tarokhian H, Jadidi-Niaragh F (2021) The molecular mechanisms and therapeutic potential of EZH2 in breast cancer. *Life Sciences* 286: 120047. doi: <https://doi.org/10.1016/j.lfs.2021.120047>
  26. Mirza Z, Ansari MS, Iqbal MS, Ahmad N, Alganmi N, Banjar H, Al-Qahtani MH, Karim S (2023) Identification of Novel Diagnostic and Prognostic Gene Signature Biomarkers for Breast Cancer Using Artificial Intelligence and Machine Learning Assisted Transcriptomics Analysis. *Cancers (Basel)* 15 (12): 3237. doi: 10.3390/cancers15123237
  27. Siegel RL, Miller KD, Wagle NS, Jemal A (2023) Cancer statistics, 2023. *CA Cancer J Clin* 73 (1): 17-48. doi: 10.3322/caac.21763
  28. Torki Z, Ghavi D, Hashemi S, Rahmati Y, Rahmanpour D, Pornour M, Alivand MR (2021) The related miRNAs involved in doxorubicin resistance or sensitivity of various cancers: an update. *Cancer Chemother Pharmacol* 88 (5): 771-793. doi: 10.1007/s00280-021-04337-8
  29. Ren L, Li J, Wang C, Lou Z, Gao S, Zhao L, Wang S, Chaulagain A, Zhang M, Li X, Tang J (2021) Single cell RNA sequencing for breast cancer: present and future. *Cell Death Discovery* 7 (1): 104. doi: 10.1038/s41420-021-00485-1
  30. Pal B, Chen Y, Vaillant F, Capaldo BD, Joyce R, Song X, Bryant VL, Penington JS, Di Stefano L, Tubau Ribera N, Wilcox S, Mann GB, Papenfuss AT, Lindeman GJ, Smyth GK, Visvader JE (2021) A single-cell RNA expression atlas of normal, preneoplastic and tumorigenic states in the human breast. *EMBO J* 40 (11): e107333. doi: 10.15252/embj.2020107333
  31. Tinker AV, Boussiotas A, Bowtell DD (2006) The challenges of gene expression microarrays for the study of human cancer. *Cancer Cell* 9 (5): 333-339. doi: 10.1016/j.ccr.2006.05.001
  32. Michiels S, Koscielny S, Hill C (2005) Prediction of cancer outcome with microarrays: a multiple random validation strategy. *Lancet* 365 (9458): 488-492. doi: 10.1016/s0140-6736(05)17866-0
  33. Li XL, Xu JH, Nie JH, Fan SJ (2012) Exogenous expression of UHRF1 promotes proliferation and metastasis of breast cancer cells. *Oncol Rep* 28 (1): 375-383. doi: 10.3892/or.2012.1792
  34. Niinuma T, Kitajima H, Kai M, Yamamoto E, Yoroza A, Ishiguro K, Sasaki H, Sudo G, Toyota M, Hatahira T, Maruyama R, Tokino T, Nakase H, Sugai T, Suzuki H (2019) UHRF1 depletion and HDAC inhibition reactivate epigenetically silenced genes in colorectal cancer cells. *Clinical Epigenetics* 11 (1): 70. doi: 10.1186/s13148-019-0668-3
  35. Kleer CG, Cao Q, Varambally S, Shen R, Ota I, Tomlins SA, Ghosh D, Sewalt RGAB, Otte AP, Hayes DF, Sabel MS, Livant D, Weiss SJ, Rubin MA, Chinnaiyan AM (2003) EZH2 is a marker of aggressive breast cancer and promotes neoplastic transformation of breast epithelial cells. *Proceedings of the National Academy of Sciences* 100 (20): 11606-11611. doi: 10.1073/pnas.1933744100
  36. Alford SH, Toy K, Merajver SD, Kleer CG (2012) Increased risk for distant metastasis in patients with familial early-stage breast cancer and high EZH2 expression. *Breast Cancer Res Treat* 132 (2): 429-437. doi: 10.1007/s10549-011-1591-2
  37. Zhang M, Chen H, Wang M, Bai F, Wu K (2020) Bioinformatics analysis of prognostic significance of COL10A1 in breast cancer. *Biosci Rep* 40 (2). doi: 10.1042/bsr20193286
  38. Zhou W, Li Y, Gu D, Xu J, Wang R, Wang H, Liu C (2022) High expression COL10A1 promotes breast cancer progression and predicts poor prognosis. *Heliyon* 8 (10): e11083. doi: <https://doi.org/10.1016/j.heliyon.2022.e11083>
  39. Sinha D, Nag P, Nanayakkara D, Duijf PHG, Burgess A, Raininga P, Smits VAJ, Bain AL, Subramanian G, Wall M, Finnie JW, Kalimutho M, Khanna KK (2020) Cep55 overexpression promotes genomic instability and tumorigenesis in mice. *Communications Biology* 3 (1): 593. doi: 10.1038/s42003-020-01304-6
  40. Tang J, Lu M, Cui Q, Zhang D, Kong D, Liao X, Ren J, Gong Y, Wu G (2019) Overexpression of ASPM, CDC20, and TTK Confer a Poorer Prognosis in Breast Cancer Identified by Gene Co-expression Network Analysis. *Front Oncol* 9. doi: 10.3389/fonc.2019.00310
  41. Xu Z, Zhang Q, Luh F, Jin B, Liu X (2019) Overexpression of the ASPM gene is associated with aggressiveness and poor outcome in bladder cancer. *Oncol Lett* 17 (2): 1865-1876. doi: 10.3892/ol.2018.9762
  42. Shang J, Zhang X, Hou G, Qi Y (2022) HMMR potential as a diagnostic and prognostic biomarker of cancer-speculation based on a pan-cancer analysis. *Front Surg* 9: 998598. doi: 10.3389/fsurg.2022.998598
  43. Matson DR, Denu RA, Zasadil LM, Burkard ME, Weaver BA, Flynn C, Stukenberg PT (2021) High nuclear TPX2 expression correlates with TP53 mutation and poor clinical behavior in a large breast cancer cohort, but is not an independent predictor of chromosomal instability. *BMC Cancer* 21 (1): 186. doi: 10.1186/s12885-021-07893-7
  44. Oshi M, Gandhi S, Huyser MR, Tokumaru Y, Yan L, Yamada A, Matsuyama R, Endo I, Takabe K (2021) MELK expression in breast cancer is associated with infiltration of immune cell and pathological compete response (pCR) after neoadjuvant chemotherapy. *Am J Cancer Res* 11 (9): 4421-4437. doi: 10.3233/ajcr-2021-11090
  45. Rivera-Rivera Y, Marina M, Jusino S, Lee M, Velázquez JV, Chardón-Colón C, Vargas G, Padmanabhan J, Chellappan SP, Saavedra HI (2021) The Nek2 centrosome-mitotic kinase contributes to the mesenchymal state, cell invasion, and migration of triple-negative breast cancer cells. *Sci Rep* 11 (1): 9016. doi: 10.1038/s41598-021-88512-0
  46. Tang N, Dou X, You X, Shi Q, Ke M, Liu G (2021) Pan-cancer analysis of the oncogenic role of discs large homolog associated protein 5 (DLGAP5) in human tumors. *Cancer Cell International* 21 (1): 457. doi: 10.1186/s12935-021-02155-9
  47. Johnsen SA, Gungör C, Prenzel T, Riethdorf S, Riethdorf L, Taniguchi-Ishigaki N, Rau T, Tursun B, Furlow JD, Sauter G, Scheffner M, Pantel K, Gannon F, Bach I (2009) Regulation of estrogen-dependent transcription by the LIM cofactors CLIM and RLIM in breast cancer. *Cancer Res* 69 (1): 128-136. doi: 10.1158/0008-5472.Can-08-1630
  48. Sklirou AD, Giannou DD, Karousi P, Cheimonidi C, Papachristopoulou G, Kontos CK, Scorilas A, Trougakos IP (2022) High mRNA Expression Levels of Heat Shock Protein Family B Member 2 (HSPB2) Are Associated with Breast Cancer Patients' Relapse and Poor Survival. *Int J Mol Sci* 23 (17). doi: 10.3390/ijms23179758
  49. Zoppino FCM, Guerrero-Gimenez ME, Castro GN, Ciocca DR (2018) Comprehensive transcriptomic analysis of heat shock proteins in the molecular subtypes of human breast cancer. *BMC*

- Cancer 18 (1): 700. doi: 10.1186/s12885-018-4621-1
50. Tian X, Wu L, Jiang M, Zhang Z, Wu R, Miao J, Liu C, Gao S (2021) Downregulation of GLYAT Facilitates Tumor Growth and Metastasis and Poor Clinical Outcomes Through the PI3K/AKT/Snail Pathway in Human Breast Cancer. *Front Oncol* 11: 641399. doi: 10.3389/fonc.2021.641399
  51. Asteriti IA, De Mattia F, Guarguaglini G (2015) Cross-Talk between AURKA and Plk1 in Mitotic Entry and Spindle Assembly. *Front Oncol* 5: 283. doi: 10.3389/fonc.2015.00283
  52. Wang B, Huang X, Liang H, Yang H, Guo Z, Ai M, Zhang J, Khan M, Tian Y, Sun Q, Mao Z, Zheng R, Yuan Y (2021) PLK1 Inhibition Sensitizes Breast Cancer Cells to Radiation via Suppressing Autophagy. *Int J Radiat Oncol Biol Phys* 110 (4): 1234-1247. doi: 10.1016/j.ijrobp.2021.02.025
  53. Ueda A, Oikawa K, Fujita K, Ishikawa A, Sato E, Ishikawa T, Kuroda M, Kanekura K (2019) Therapeutic potential of PLK1 inhibition in triple-negative breast cancer. *Laboratory Investigation* 99 (9): 1275-1286. doi: 10.1038/s41374-019-0247-4
  54. Ding K, Li W, Zou Z, Zou X, Wang C (2014) CCNB1 is a prognostic biomarker for ER+ breast cancer. *Med Hypotheses* 83 (3): 359-364. doi: 10.1016/j.mehy.2014.06.013
  55. Li B, Zhu HB, Song GD, Cheng JH, Li CZ, Zhang YZ, Zhao P (2019) Regulating the CCNB1 gene can affect cell proliferation and apoptosis in pituitary adenomas and activate epithelial-to-mesenchymal transition. *Oncol Lett* 18 (5): 4651-4658. doi: 10.3892/ol.2019.10847
  56. Xie YG, Yu Y, Hou LK, Wang X, Zhang B, Cao XC (2016) FYN promotes breast cancer progression through epithelial-mesenchymal transition. *Oncol Rep* 36 (2): 1000-1006. doi: 10.3892/or.2016.4894
  57. Mohammed S, Shamseddine AA, Newcomb B, Chavez RS, Panzner TD, Lee AH, Canals D, Okeoma CM, Clarke CJ, Hannun YA (2021) Sublethal doxorubicin promotes migration and invasion of breast cancer cells: role of Src Family non-receptor tyrosine kinases. *Breast Cancer Research* 23 (1): 76. doi: 10.1186/s13058-021-01452-5
  58. Liu X, Liu Y, Wang Q, Song S, Feng L, Shi C (2021) The Alterations and Potential Roles of MCMs in Breast Cancer. *J Oncol* 2021: 7928937. doi: 10.1155/2021/7928937
  59. Liu S, Ye Z, Xue VW, Sun Q, Li H, Lu D (2023) KIF2C is a prognostic biomarker associated with immune cell infiltration in breast cancer. *BMC Cancer* 23 (1): 307. doi: 10.1186/s12885-023-10788-4
  60. Zhu P, Liu G, Wang X, Lu J, Zhou Y, Chen S, Gao Y, Wang C, Yu J, Sun Y, Zhou P (2022) Transcription factor c-Jun modulates GLUT1 in glycolysis and breast cancer metastasis. *BMC Cancer* 22 (1): 1283. doi: 10.1186/s12885-022-10393-x
  61. Wu D, Han B, Guo L, Fan Z (2016) Molecular mechanisms associated with breast cancer based on integrated gene expression profiling by bioinformatics analysis. *Journal of Obstetrics and Gynecology* 36 (5): 615-621. doi: 10.3109/01443615.2015.1127902
  62. Trabert B, Sherman ME, Kannan N, Stanczyk FZ (2020) Progesterone and Breast Cancer. *Endocr Rev* 41 (2): 320-344. doi: 10.1210/endrev/bnz001
  63. Dong H, Claffey KP, Brocke S, Epstein PM (2015) Inhibition of breast cancer cell migration by activation of cAMP signaling. *Breast Cancer Res Treat* 152 (1): 17-28. doi: 10.1007/s10549-015-3445-9
  64. Zhang H, Kong Q, Wang J, Jiang Y, Hua H (2020) Complex roles of cAMP-PKA-CREB signaling in cancer. *Experimental Hematology & Oncology* 9 (1): 32. doi: 10.1186/s40164-020-00191-1
  65. Aronica SM, Kraus WL, Katzenellenbogen BS (1994) Estrogen action via the cAMP signaling pathway: stimulation of adenylylate cyclase and cAMP-regulated gene transcription. *Proceedings of the National Academy of Sciences* 91 (18): 8517-8521. doi: 10.1073/pnas.91.18.8517
  66. Silva CID, Gonçalves-de-Albuquerque CF, Moraes BPTd, Garcia DG, Burth P (2021) Na/K-ATPase: Their role in cell adhesion and migration in cancer. *Biochimie* 185: 1-8. doi: https://doi.org/10.1016/j.biochi.2021.03.002
  67. Hong SH, Goh SH, Lee SJ, Hwang JA, Lee J, Choi IJ, Seo H, Park JH, Suzuki H, Yamamoto E, Kim IH, Jeong JS, Ju MH, Lee DH, Lee YS (2013) Upregulation of adenylylate cyclase 3 (ADCY3) increases the tumorigenic potential of cells by activating the CREB pathway. *Oncotarget* 4 (10): 1791-1803. doi: 10.18632/oncotarget.1324
  68. Feschenko MS, Donnet C, Wetzel RK, Asinowski NK, Jones LR, Sweadner KJ (2003) Phospholemman, a single-span membrane protein, is an accessory protein of Na,K-ATPase in cerebellum and choroid plexus. *J Neurosci* 23 (6): 2161-2169. doi: 10.1523/jneurosci.23-06-02161.2003